Journal of Applied Mechanics and Technical Physics, Vol. 35, No. 3, 1994

EVAPORATIVE MECHANISM OF CLUSTER GENERATION BY A SOLID SURFACE BOUNDED BY VAPOR

A. A. Bochkarev and M. V. Pukhovoi

UDC 53.03+536.422.4:539.211

The formation of free microscopic particles has been observed in experiments involving the vacuum dispersion of zinc vapor on a graphite substrate. Mathematical modeling of the growth of condensate nuclei on the surface has shown that there is a supersaturation region in which growth of the nuclei is accompanied by evaporation at their base. Such evaporation might lead to loss of contact between the nucleus and the substrate. A study was made of certain laws governing this phenomenon. The evaporative generation of clusters might be an important component of the mechanism by which smoke is formed.

Specialists whose job entails working with vacuum heat treatment units know well that some dust is formed in the vacuum system when the treatment being administered is performed at temperatures at which significant evaporation of some component or components of the unit occurs. Such dust generation usually complicates the operation of the system and requires its periodic cleaning, along with the introduction of vacuum pumps. It is known from general considerations that the dust is formed as a result of the condensation of vapors generated by the high-temperature elements of the unit. However, the mechanism and principles underlying this phenomenon have yet to be fully investigated.

The generation of free clusters of roughly critical size by a solid surface bounded by vapor was first detected in [1]. The following was observed in this case. Heat of condensation was continuously liberated on the condensation surface, but condensate that was fixed to the substrate was not formed. A substrate that had previously been dusted by discrete condensate nuclei was cleaned spontaneously several seconds after the flow of vapor was cut off. Clusters of a condensed phase (magnesium) about 1 nm in size were deposited on grids prepared for electron microscope studies performed with carbon films that were turned toward the substrate and closed off from the vapor flow. The authors of [2, 3] observed the generation of clusters of aluminum containing about 20 atoms by the surface of the heated nozzle of an evaporator. A fluctuation mechanism was proposed in [4] to explain the separation of ultrasmall particles from a condensation surface. The conditions necessary for the transfer of all condensate nuclei from the surface to the vapor phase was determined in relation to the size of the nuclei and the energy of their bond with the substrate.

There is little doubt that the fluctuation mechanism is responsible for the separation of microparticles containing a small number of atoms, which in turn means that the generation of free particles by a solid surface has been reliably established for high degrees of supersaturation of the vapor relative to the substrate. The issues of the range of supersaturation in which such particles are generated and the possible mechanism of generation at low levels of supersaturation will be taken up in the present investigation.

1. EXPERIMENT

Figure 1 presents a sketch of the experimental setup. Zinc vapor passes from evaporator 1 [1], with the evaporation point T_v, through a long graphite nozzle 2 of radius $R = 9\cdot 10^{-3}$ m, with the temperature T_0, into a vacuum chamber with a vacuum pressure of $5\cdot 10^{-5}$ Pa. A glass-graphite beaker 3 with the temperature T_s is located 0.28 m from the nozzle. A movable baffle 5 which spans the vapor flow and a diaphragm 4 are positioned between the beaker and nozzle. A collimator 6 with a polished brass diaphragm-transducer 7 and the crystal of a quartz balance 8 are located 0.1 m from the beaker at a 40° angle to its axis. The signal generated in the transducer by the particles which strike it is sent to a selective nanovoltmeter through a filter which cuts off harmonics that are multiples of 50 Hz.

Novosibirsk. Translated from Prikladnaya Mekhanika i Tekhnicheskaya Fizika, Vol. 35, No. 3, pp. 102-111, May-June, 1994. Original article submitted July 2, 1993; revision submitted July 20, 1993.

TABLE 1

Series of experiments	Position of baffle	T_v	T_0	T_s	I, rel. un.	Condition of target before the measurements	Type of condensate on the target after the measurements
		K					
1	Open	690	735	525	6,1		Columnar structures, characteristic size 0.1 μm
		690	735	539	12,4		
		690	735	559	10,8		
		687	758	567	13,8		
2	Open	687	758	623	4,7	Coated at $T_s \leq 453$ K	Cleaning of the surface
	Closed	687	758	623	11,7		

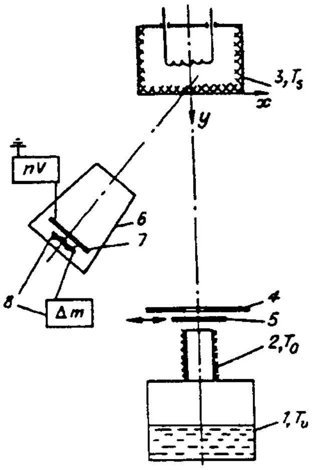

Fig. 1

The arrival of a signal from the transducer coincides with the change in the rate of increase in mass on the quartz balance. The peak signals formed in the nanovoltmeter can be resolved relative to the noise level (signal/noise ratio greater than two). A peak signal can be formed for several reasons when particles strike the transducer: the electric potential on the transducer is different from the potential of the free particles; the electric double layer at the boundary of contact between a particle and the transducer surface undergoes restructuring at the moment contact occurs. The most reliable reproducible data was obtained when an electric potential was supplied to the target (beaker) and the sensitivity of the nanovoltmeter was limited by narrowing the transmission band.

Experiments were conducted with constant temperatures on the evaporator T_v = 687-691 K and nozzle T_0 = 737-741 K and variation of the temperature of the target T_s. This situation corresponded to supersaturation of the target relative to the flow of zinc vapor incident on it. The signals from the transducer were measured with the baffle in both positions, which either allowed the vapor flow to pass to the beaker or cut the flow off.

Measurements made with a target temperature of 288-303 K showed that no zinc was deposited on the target in this case. No signal resolvable at the given noise level was recorded on the nanovoltmeter. The absence of condensation on the target indicates that the phenomenon of condensation "breakdown" (disruption) observed in [5, 6] occurred. The presence of the low-temperature "breakdown" region is related to the adsorption of impurities in the vapor (vacuum oil), which in this case leads to a significant reduction in the percentage of free adsorption vacancies and surface concentration of zinc atoms. The latter in turn leads to a decrease in effective supersaturation, a reduction in the rate of condensation, and the breakdown of condensation [7]. Stable condensation of zinc on the target occurs only when target temperature is within the range 303-523 K.

Measurements made with a target temperature >525 K showed the presence on the transducer of signals that could be reliably separated from the noise even when there was no electric potential on the target. The pulse signals recorded by the nanovoltmeter were accompanied by an irreversible increase in mass on the balance. Table 1 shows characteristics of the regimes in which microscopic particles of the condensed phase were observed to have reached the transducer. Figure 2 shows a bright-field photograph (3000×) of particles that reached the transducer. It is apparent that the captured particles have dimensions of 0.3-0.5 μm and are commensurate with the characteristic size of the columnar structures formed when

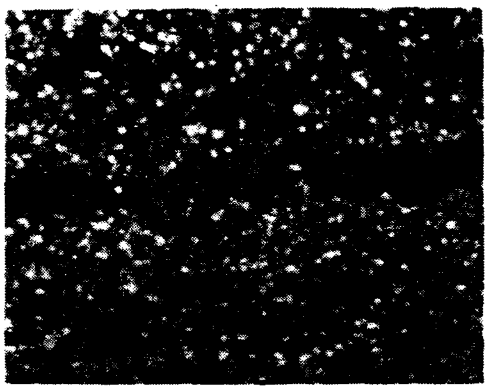

Fig. 2

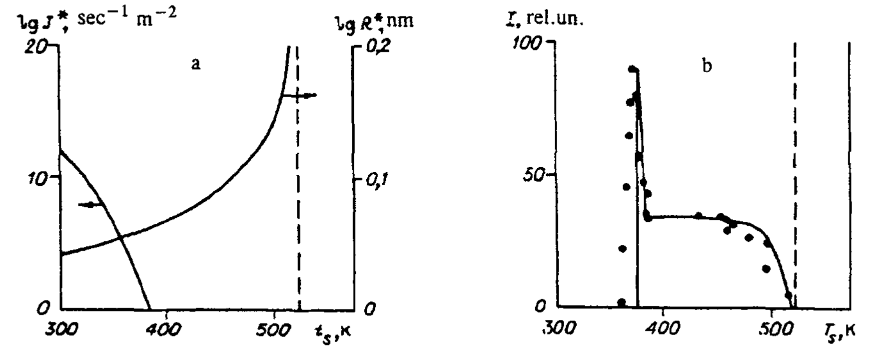

Fig. 3

condensation takes place on the surface of the target. A signal was generated by the arrival of clusters at the transducer in the second series of experiments (see Table 1) only when columnar structures of condensate had previously been formed on the surface of the glass-graphite. In this case, the vapor flow could have been partially cut off by the baffle.

Figure 3b shows the results of measurements of the signals on the transducer with a target potential of 30 V and transmission band of 70-90 Hz. The data is shown in relative units and is represented by different points as a function of target temperature. These measurements were made with the baffle open (allowing the flow to proceed to the target). The vapor source was the same as previously, and the target was periodically cleaned by raising the temperature.

Thus, the experimental results showed that the condensation of zinc vapor on the surface of a glass-graphite substrate and the associated formation of dispersed columnar structures are accompanied by the emission of microscopic particles whose characteristic size correlates with the characteristic dimensions of the condensate structures. This finding is sufficient to establish the direction and level of modeling of the given phenomenon, i.e. the probability of the separation of microparticles of condensate from the surface in the course of local evaporation.

2. Mathematical Modeling of the Evolution of Nuclei. The process by which the shape of the condensate nuclei evolves is controlled by several factors: convective and radiative heat transfer, the movements of the incident and secondary vapor flows, the surface migration of adatoms. It is not especially difficult to calculate heat transfer when condensation takes place in a vacuum and involves the formation of dispersed condensates in which the crystallites are much smaller than the mean free path of atoms in the vapor phase. The fraction of convective heat transfer occurring at the condensation front is determined by the excess thermal energy of the vapor — which is calculated from the difference between the temperatures of the vapor and the substrate. Radiative heat transfer can be calculated if we know the distribution of temperature and optical properties in the system formed by the condensation front and the surrounding space. The thermal state of the substrate and conductive properties of the condensate must be considered when the temperature of the condensation front is calculated. The vapor flow incident on the front must be calculated using the initial parameters of the flow, which are in turn determined by the parameters of the source of vapor and conditions in the medium surrounding the substrate. The evaporation of the surface of the condensate depends on local temperature and the curvature of this surface. Surface migration can be computed if we know the local temperature on the condensation front and assign some type of boundary conditions. Each of the factors mentioned above has been thoroughly investigated individually, and there are well-known algorithms for formulating and solving various problems.

However, using the same algorithms to describe the evolution of nuclei on the condensation front is difficult not only because all of these factors are interrelated and must be calculated simultaneously with variable boundary conditions, but also because the local physical properties of the surfaces — accomodation coefficient, adhesion coefficient, emissivity, and emittance — are difficult to determine. Thus, at present the evolution of the condensation front can only be modeled numerically using several assumptions. We will make use of the following assumptions:

a) all of the local physical properties of the surfaces (accomodation and adhesion coefficients, emissivity, emittance) are equal to unity;

b) we ignore surface migration because we are studying the evolution of crystallites separated by spaces on the substrate where condensation does not occur;

c) conductive heat transfer from the condensation front to the substrate is calculated in a quasi-unidimensional approximation without allowance for temperature gradients along the substrate.

Given these assumptions, we can write the following equation for the local heat flux on an element of the condensation surface

$$\begin{aligned}\delta q = {} & \sigma\varepsilon_{y}\int_{C}\varepsilon_{c}(T_{c}^{4} - T_{y}^{4})dC + \\ & + \sigma\varepsilon_{y}\int_{S}\varepsilon_{0}(T_{0}^{4} - T_{y}^{4})dS + (\alpha_{y}L + c_{V}(T_{0} - T_{y}))\int_{S} j_{0}dS + \\ & + (\alpha_{y}L + c_{V}(T_{y_i} - T_{y}))\int_{K} j_{\alpha}dK + c_{m}(T_{m} - T_{y})\int_{C} j_{m}dC - LJ_{v},\end{aligned} \tag{2.1}$$

where ε_y, ε_c, and ε_0 are the emissivities of the crystallite, vacuum chamber, and vapor source, respectively; T_y, T_c, and T_0 are their temperatures; σ is the Stefan—Boltzmann constant; L and c_V are the heat of condensation and heat capacity of the vapor; c_m, T_{ime}, and j_m are the heat capacity, temperature, and flux of impurity vapors from an element of space; J_v is the unit flow due to vaporization (flux of zinc vapor); α_c is the local condensation coefficient. The first and second terms of the equation account for heat radiation from the chamber walls and the vapor source, the third term accounts for the heat of condensation and heat convection from the source vapor that reaches the substrate, the fourth term represents the convective flow of heat from adjacent crystallites, the fifth term represents convective heat exchange with impurity vapor components, and the sixth term accounts for heat losses due to local evaporation of the crystallites. In a quasi-unidimensional, quasisteady approximation, the integral of heat flux in a crystallite from the apex to a specified cross section determines the temperature gradient over the height of the crystallite:

$$\int_{F_e}\delta q dF_{e} = \lambda_{y}F_{y}(y)\,(dT_{y}/dy). \tag{2.2}$$

Here, λ_y is the thermal conductivity of the crystallite; F_y is the cross-sectional area of the crystallite in a plane perpendicular to the y axis; F_e is the area of the lateral surface from the given section to the apex of the crystallite.

Replacement of the left side of (2.2) by (2.1) yields an integrodifferential equation for the local temperature of the crystallite surface.

We can write the below equation of local mass transfer for the local normal rate of increase in the surface of the crystallite

$$dr/dt = \omega_{a}\left(\alpha_{y}\int_{S} j_{s}dS + \alpha_{y}\int_{K} j_{y_i}dK - J_{v}\right). \tag{2.3}$$

System (2.2)-(2.3) links the evolution and thermal state of a crystallite grown by condensation from vapor.

In light of the absence of reliable analytical solutions for the above equations, we propose the following for their numerical solution. The initial approximation is established by solving the system of equations that describes the kinetics of sorption processes and choosing the structure of the system of nuclei formed on the substrate as shown in [8]. After local vapor flow is calculated for this configuration with artificially assigned condensation coefficients, we calculate the distribution of temperature over the surface of the crystallites. The system of kinetic equations for sorption is solved, the condensation coefficients are found, and the flows of reevaporated substances are refined. If the calculated condensation coefficients do not correspond to the assigned coefficients, the estimates need to be refined iteratively. After a satisfactory level of accuracy is

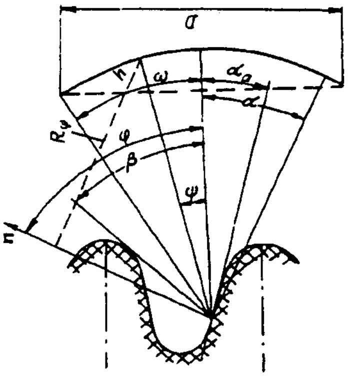

Fig. 4

achieved, we calculate the local increments of the surface of the crystallites for a specified time interval. Naturally, the proposed algorithm involves a large amount of calculation, which probably accounts for the fact that very few solutions of such problems have yet been attempted. For our purposes here — where we need to examine only characteristic features of the evolution of condensate nuclei with low levels of supersaturation and a high vacuum — it is sufficient to perform calculations for the isothermal case with an assigned condensation coefficient equal to unity.

We assume that the vapor source is a spherical segment of diameter D with its center at a point at which vapor flux is to be calculated. Such a representation of the source is convenient because it makes it possible to vary the angle of the segment and thus model different sources — from point sources to a half-space — without restructuring the formulas. Figure 4 depicts the scheme employed to calculate the characteristic angles.

No shadowing occurs on the section of the condensation surface where the entire surface of the source is completely visible, while vapor flux on the section normal to the axis of the source can be determined from the formula

$$J = J_0(1 - \sin^2(\pi/2 - \omega))$$

(J_0 is the flux of vapor from the surface of the source and ω is the half-angle of the spherical sector of source visibility). If a normal to a section of the condensation surface makes the angle φ with the axis of the source, then the vapor flux on the section

$$J_y = J_0(1 - \sin^2(\pi/2 - \omega))\cos\varphi. \tag{2.4}$$

When a group of crystallites is being modeled, there may arise a situation in which part of the flow of vapor from the source is shadowed by adjacent crystallites. Since an exact calculation of this shadowing requires knowledge of the position and form of these crystallites and since such a three-dimensional calculation would be extremely involved, we will assume that the adjacent crystallites are of the same form as the crystallite being analyzed and that, on the average, the crystallites are located the same distance from the source. In this case, to calculate the shadow effect it is convenient to assume that the contours of the adjacent crystallites create a circular shadowing of a given point over the solid half-angle β. Then the flux on an area of the crystallite in question can be calculated from the formula

$$J_y = J_0(1 - \sin^2(\pi/2 - \beta))\cos\varphi. \tag{2.5}$$

Equation (2.5) means that the shadowing by adjacent crystallites reduces the diameter of the source visible from the point being analyzed. It should be noted that calculating with (2.5) yields a certain error when the neighbors are close together. This is true even of the case when they are positioned symmetrically relative to the crystallite being examined if the given point is not on the axis of the crystallite.

In the case where the source is shadowed by the body of the crystallite being analyzed, we assume that a part of the source bounded by a section of large diameter tangent to the body of the crystallite is visible from the point of observation. For convex crystallites, this is a plane that is tangent to the surface of the crystallite at the observation point and makes the angle α with the axis of the source.

TABLE 2

Character of shadowing	Conditions	Formula	Parameters
No shadowing	$\alpha_1 < \alpha, \alpha < -\omega, \beta > \omega$	(2.4)	
Shadowing by a neighbor	$\alpha_1 < \alpha, \alpha < -\omega, \beta < \omega$	(2.5)	
Shadowing by the crystallite itself	$\alpha_1 < \alpha, \alpha > -\omega, \beta > \omega, \omega - \alpha < \pi/2$	(2.6)	$\psi_1 = 0, \beta_1 = \omega,$ $\psi_2 = \omega - \alpha$
	$\alpha_1 < \alpha, \alpha > -\omega, \beta > \omega, \omega - \alpha > \pi/2$	(2.8)	$\psi_1 = 0, \beta_1 = \omega,$ $\psi_2 = \pi - \omega + \alpha$
Shadowing by a neighbor and the crystallite itself	$\alpha_1 < \alpha, \alpha > -\omega, \beta < \omega, \beta - \alpha < \pi/2$	(2.6)	$\psi_1 = 0, \beta_1 = \beta,$ $\psi_2 = \beta - \alpha$
	$\alpha_1 < \alpha, \alpha > -\omega, \beta < \omega, \beta - \alpha > \pi/2$	(2.8)	$\psi_1 = 0, \beta_1 = \beta,$ $\psi_2 = \pi - \beta + \alpha$
No shadowing	$\alpha_1 > \alpha, \alpha_1 < -\omega, \beta > \omega$	(2.4)	
Shadowing by a neighbor	$\alpha_1 > \alpha, \alpha_1 < -\omega, \beta < \omega$	(2.5)	
Shadowing by the apex of the crystallite	$\alpha_1 > \alpha, \alpha_1 > -\omega, \beta > \omega, \omega - \alpha < \pi/2$	(2.6)	$\psi_1 = \alpha_1 - \alpha,$ $\beta_1 = \omega,$ $\psi_2 = \omega - \alpha$
	$\alpha_1 > \alpha, \alpha_1 > -\omega, \beta > \omega, \omega - \alpha > \pi/2$	(2.8)	$\psi_1 = \alpha_1 - \alpha,$ $\beta_1 = \omega,$ $\psi_2 = \pi - \omega + \alpha$
Shadowing by the apex of the crystallite and a neighbor	$\alpha_1 > \alpha, \alpha_1 > -\omega, \beta < \omega, \beta - \alpha < \pi/2$	(2.6)	$\psi_1 = \alpha_1 - \alpha,$ $\beta_1 = \beta,$ $\psi_2 = \beta - \alpha$
	$\alpha_1 > \alpha, \alpha_1 > -\omega, \beta < \omega, \beta - \alpha > \pi/2$	(2.8)	$\psi_1 = \alpha_1 - \alpha,$ $\beta_1 = \beta,$ $\psi_2 = \pi - \beta + \alpha$

It is convenient to integrate vapor flux on the analyzed section of the crystallite surface over sections of the visible surface of the source by means of planes that are parallel to the plane tangent to the body of the crystallite at the observation point. If ψ and θ are the azimuthal and meridional angles of points of the evaporator visible from the point of observation, we can calculate an element of the surface of the source $dF = Rd\psi R_\psi d\theta$, where $R_\psi = R\cos\psi$ is the radius of rotation of the integrated element. We can also calculate the elementary flux of vapor mm source $dJ_\Sigma = J_0R^2d\theta\cos\psi$ and an element of the normal projection of the vapor flux to a section of the crystallite surface. $dJ_{\Sigma c} = J_0R^2d\theta\sin\psi\cos\psi d\psi$. Since integration over θ is performed by rotation about a normal to the tangent plane with ψ constant, then

$$dJ_{\Sigma y} = J_0R^2\int_{\psi_1}^{\psi_2} \theta_a \sin\psi \cos\psi d\psi$$

(the normal vapor flux),

$$J_x = (J_0/\pi) \int_{\psi_1}^{\psi_2} \theta_a \sin\psi \cos\psi d\psi \tag{2.6}$$

(the normal flux to a local section of the crystallite surface). Here, $\theta_a = 4\arctan(2h/a)$ is the length (in radians) of the arc described by the element of the integrated surface with rotation about the normal. It is calculated using the equation

$$h = R(\cos(\psi + \alpha) - \cos\beta_1)/\cos\alpha,\ a = 2(2hR\cos\psi - h^2)^{1/2} \tag{2.7}$$

(h being the height and a the chord of the segment of the vapor source in the plane of integration).

The limits of integration in (2.6) are calculated differently for convex crystallites for different cases of shadowing:

if $\beta > \omega$ and $\omega - \alpha < \pi/2$, then $\psi_1 = 0, \psi_2 = \omega - \alpha$, while in (2.7) $\beta_1 = \omega$;

if $\beta < \omega$ and $\beta - \alpha < \pi/2$, then $\psi_1 = 0, \psi_2 = \beta - \alpha$, while in (2.7) $\beta_1 = \beta$.

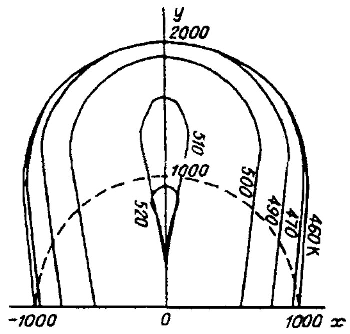

Fig. 5

Two other cases are possible at $\omega > \pi/4$, when part of integral (2.6) can be taken in quadratures

$$J_y = J_0(1 - \sin^2\psi_2) + (J_0/\pi)\int_{\psi_1}^{\psi_2} \theta_a \sin\psi \cos\psi d\psi, \tag{2.8}$$

where

if $\beta > \omega$ and $\omega - \alpha > \pi/2$, then $\psi_1 = 0$, $\psi_2 = \pi - \omega$ – while in (2.7) $\beta_1 = \omega$;
if $\beta < \omega$ and $\beta - \alpha > \pi/2$, then $\psi_1 = 0$, $\psi_2 = \pi - \beta$ – while in (2.7) $\beta_1 = \beta$.

For concave-convex crystallites, when shadowing occurs as a result of the apex of the crystallite being considered, there is a change in the lower limit in integrals (2.6) and (2.8) $\psi_1 = \alpha_1 - \alpha$ (where α_1 is the angle between the axis of the source and a plane which passes through the given point and is tangent to the apex of the crystallite). Table 2 shows formulas and parameters used to calculate vapor flux on the surface of crystallites. The results represent somewhat of an overestimate, given the assumption of shadowing by the apex as a plane, but the calculations are much simpler in this instance.

Figure 5 shows results of calculation of the profiles of crystallites formed by condensation from a half-space onto nuclei located 50 nm from one another on the substrate. Also shown for comparison are profiles of roughly the same height obtained with different substrate temperatures. The flow of vapor reflected from the substrate was not taken into account in the latter calculations, such conditions corresponding to the evolution of nuclei formed on projections on a substrate with microroughness. It is evident from Fig. 5 that, with an increase in substrate temperature, reevaporation leads to a reduction in the size of the base of the crystallites. The base evaporates completely at a substrate temperature of 508 K and the crystal loses contact with the substrate.

Two important conclusions follow from these results. First of all, the supersaturation calculated from the parameters of the vapor flow, substrate temperature, and nuclei curvature is not sufficient for growth of the nuclei. The sections of the nucleus surface shadowed from the flow by the apex may turn out to be unsaturated. This means that it is necessary to more precisely account for the properties of the substrate when nucleation processes are being calculated in order to determine supersaturation. Secondly, the results obtained here indicate that free microparticles may be generated by nucleation on a solid surface and subsequent loss of contact with that surface due to evaporation of their base. The mechanism of this phenomenon is fundamentally different from the previously discovered fluctuation mechanism of free cluster generation [4].

3. Interpretation of Empirical Data. To make a comparison with the experimental data, we can construct an approximate theoretical model of the emission of microparticles from a solid surface by the evaporation mechanism. After finding the vapor flow reaching a nucleus

$$J_f = (1 - \sin^2(\pi/2 - \omega))p_{hi}/(2\pi m_a kT_i)^{1/2}$$

and the flow evaporated from the same nucleus

$$J_e = (p_{hs}/(2\pi m_a kT_s)^{1/2}) \exp(2\gamma\omega_a/kT_s R^*)$$

we can determine the radius of the curvature of the critical nucleus:

$$R^* = 2\gamma\omega_a/k/T_s\ln(J_f/J_v).$$

A critical nucleus with the curvature $2/R^*$ and contact angle φ has the volume $V = \pi R^{*3}(2/3 - \cos\varphi + \cos^3\varphi/3)$ and consists of $N = V/\omega$ atoms. The energy barrier to formation of the nucleus $\delta\Phi(N) = 4\pi\omega_a{}^2\gamma^3(1 - \cos\varphi)^2(2 + \cos\varphi)/3(kT_s)^2\ln^2(J_f/J_v)$ [8]. The concentration of subcritical aggregates on the substrate is determined as in [9] $n(N) = n_a\exp(\delta\Phi(N)/kT_s)$ (n_a is the density of adsorption vacancies). The frequency of heterogeneous nucleation is found from the formula [10] $J^* = (\zeta\xi\nu n(N)/n_a)\cdot\exp(-U_D/kT_s)$, where ζ is the fraction of peripheral adsorption supplying the nucleus with adatoms; $\xi = (J_f/\nu)\exp(\varepsilon_s/kT_s)$ is the surface concentration of adatoms on the substrate in accordance with the Langmuir adsorption isotherm; ν is the frequency of thermal vibration of the adatoms; ε_s is the energy of the bond of the adatoms with the substrate; $U_D \cong 0.3\varepsilon_s$ is the energy of activation of surface diffusion. We calculated the energy for the bonding of zinc adatoms and a graphite substrate by means of Young's formula $\varepsilon_s/\varepsilon_1 = (1 + \cos\varphi)/2$ (where ε_1, the energy for the bonding of zinc adatoms to a zinc substrate, is roughly 1/6 the atomic latent heat of vaporization: $\varepsilon_1 = 9.54\cdot10^{-20}$ J).

Figure 3a shows the results of calculation of the frequency of nucleation and radius of curvature of critical zinc nuclei on a graphite substrate with the contact angle $\varphi = \pi/2$ under conditions corresponding to the above experiment. It is evident that the appearance of a signal from the arrival of microparticles at the transducer corresponds roughly to a decrease in the frequency of nucleation to values on the order of 10^2 m^{-2}sec^{-1}. Considering that the measurements were obtained with a transmission band of 70-90 Hz, we can conclude that the surge in the signal recorded in the experiment is formed in the region of substrate temperatures in which microparticles emitted by the substrate generate a signal on the transducer whose frequency coincides with the transmission frequency. The absence of a signal at temperatures to the left of the surge does not mean that no such emission takes place. The character of the signal at temperatures to the right of the surge — where almost no nucleation occurs — indicates that the signal was generated as a result of factors not having to do with nucleation.

In the substrate temperature range 370-520 K, where the frequency of nucleation $J^* < 1$ m^{-2}sec^{-1}, zinc condensation is governed by capillary effects. Zinc condensate nuclei can be formed in depressions in the microroughness of the graphite substrate with concave menisci without overcoming a nucleation energy barrier. As the depressions are filled, the contact angle $\cong \pi/2$ results in the appearance of convexity in the nuclei formed by capillary condensation. The limiting curvature of such nuclei conforms to the curvature of the critical nucleus at the corresponding temperature. As the curvature of capillary nuclei approaches the critical value, they too may leave the substrate as a result of evaporation of the side opposite the vapor flow. If we assume that the surface concentration of capillary nuclei is proportional to the surface concentration of capillary defects in the substrate (i.e., is constant for the given substrate) and is proportional to nucleus growth rate and if we also suppose that their lifetime on the substrate is proportional to the transverse dimension divided by the rate of evaporation, then the flow of microparticles emitted within the given substrate temperature interval is determined by the formula

$$J_y \simeq J_v(J_f - J_v)/R^*.$$

If we also assume that each microparticle transfers from the substrate to the transducer a charge that is proportional to its size, we obtain the following to describe the signal on the transducer in the substrate temperature region in which nucleation is absent

$$I \simeq J_v(J_f - J_v).$$

By applying similar logic to critical nuclei in the substrate temperature region in which nucleation is substantial, we can construct an expression to describe the signal in this interval as well. Derivation of this formula is simplified by knowledge of the frequency of nucleation. The general formula for describing the signal throughout the investigated temperature range has the form $I \simeq J^*J_v + \eta J_v(J_f - J_v)$, where the proportionality factor η, including the electric constants and the surface density of capillary defects in the substrate, can be chosen by comparison with experimental results. The solid line in Fig. 3b shows the results of calculation of I with the condition that signal frequency be limited to 100 Hz on account of the instruments employed.

Proceeding on the basis of the agreement between the theoretical and experimental results for the signal, we will calculate the distribution function for the particles emitted from the surface. Such a calculation can be performed if the supersaturation for supercritical nuclei is inserted into the formula for the energy barrier.

The results of calculations of the distribution functions f of particles formed by nucleation (dashed line) and emitted into the vapor phase (solid line) are shown in Fig. 6a, and b, for the temperatures characteristic of the regions of developed nucleation and capillary nucleation. It is apparent that the spectrum of dimensions of the particles emitted within the nucleation region is close to the dimensional spectrum for particles formed by capillary action. The range of dimensions of the particles

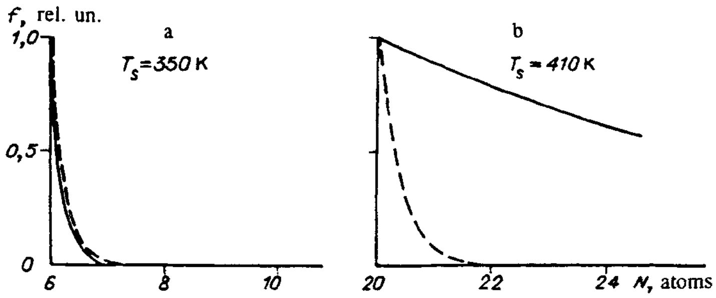

Fig. 6

emitted is broader in the region where nucleation is insignificant. At target temperatures >520 K, where supersaturation is not achieved, the dimensional spectrum of the emitted particles is determined by the characteristic dimension of the condensate particles that were heated to these temperatures along with the target. The size of the particles emitted in this case is approximately 0.1 μm.

4. Discussion of the Results. The above-discussed phenomenon of the evaporative removal of microscopic particles from a solid surface is of interest to researchers studying nucleation and the initial stage of condensation. The fact that condensate nuclei of near-critical size are the nuclei most likely to leave the surface is important for the surface concentration of nuclei and has the effect of retarding the coverage of the substrate with condensate. In reality, a decrease in the surface concentration of nuclei increases the degree of supersaturation necessary for the beginning of condensation and causes the results calculated on the basis of classical nucleation theories to deviate from the empirical data. Thus, the work done in this article is an attempt to make certain corrections to theories of nucleation.

The generation of free microparticles by the mechanism described above might be a significant factor in the formation of smoke. There are two key aspects to this mechanism: the action of a source of smoke particles that is in addition to the homogeneous source; the action of a source of condensation centers for the formation of smoke particles. Future studies of this question should be oriented toward determining the conditions which hinder the development of the given phenomenon.

The study described here was completed with the financial support of the Soros Fund for research into "the collective growth of crystallites from a vapor phase and the structure of condensates," and the "simultaneous condensation of vapors of mutually insoluble substançe."

REFERENCES

1. A. A. Bochkarev, A. S. Zolkin, and Yu. G. Shukhov, "Differential thermal analysis of a stream of vapors of metals," in: Boiling and Condensation (Hydrodynamics and Heat Transfer) [in Russian], Nauka, Novosibirsk (1986).
2. W. Knauer, "Formation of large metal clusters by surface nucleation," J. Appl. Phys., **63**(3) (1987).
3. J. H. Hawley and P. J. Ficalora, "Heterogeneous formation of small aluminum clusters," J. Appl. Phys., **63**(8) (1988).
4. A. A. Bochkarev, A. N. Polishchuk, and V. I. Polyakova, "Generation of free ultrasmall particles by a solid surface bounded by vapor," Izv. Sib. Otd. Akad. Nauk SSSR, Fiz. Tekh. Zh., No. 2 (1993).
5. L. S. Palatnik and Yu. F. Komnik, "Critical temperature for the condensation of Bi, Pb, and Sn," Fiz. Met. Metalloved., **60**, No. 4 (1960).
6. L. S. Palatnik and N. T. Gladkikh, "Conditions of condensation of Zn and Cd in the second boundary region of temperatures," Fiz. Tverd. Tela, **4**, No. 2 (1962).
7. A. A. Bochkarev, V. I. Polyakova, and Yu. G. Shukhov, "Effect of sorption processes in the residual atmosphere on the heterogeneous condensation of vapors of metals," in: Thermophysics of the Crystallization and High-Temperature Treatment of Materials [in Russian], IT SO An SSSR (Institute of Thermophysics, Siberian Branch of the Academy of Sciences of the USSR), Novosibirsk (1991).
8. A. A. Bochkarev and V. I. Polyakova, "Genetics and evolution of the structures of vacuum condensates," Preprint. IT SO An SSSR, Novosibirsk (1993).
9. L. D. Landau and E. M. Lifshitz, Statistical Physics [in Russian], Vol. 1, Nauka, Moscow (1976).
10. A. A. Chernov, E. I. Givargizov, Kh. S. Bogdasarov, et al., Modern Crystallography [in Russian], Vol. 3, Nauka, Moscow (1980).